JACC: CARDIOVASCULAR IMAGING VOL. 4, NO. 12, 2011

ISSN 1936-878X/$36.00
PUBLISHED BY ELSEVIER INC. DOI:10.1016/j.jcmg.2011.09.013

CT for Evaluation of Myocardial Cell Therapy in Heart Failure

A Comparison With CMR Imaging

Karl H. Schuleri, MD,* Marco Centola, MD,*† Seong Hoon Choi, MD, PhD,*‡
Kristine S. Evers, BS,* Fady Dawoud, PhD,* Richard T. George, MD,*
João A. C. Lima, MD,* Albert C. Lardo, PhD*§

Baltimore, Maryland; Milan, Italy; and Uslan, South Korea

OBJECTIVES The aim of this study was to use multidetector computed tomography (MDCT) to assess therapeutic effects of myocardial regenerative cell therapies.

BACKGROUND Cell transplantation is being widely investigated as a potential therapy in heart failure. Noninvasive imaging techniques are frequently used to investigate therapeutic effects of cell therapies in the preclinical and clinical settings. Previous studies have shown that cardiac MDCT can accurately quantify myocardial scar tissue and determine left ventricular (LV) volumes and ejection fraction (LVEF).

METHODS Twenty-two minipigs were randomized to intramyocardial injection of phosphate-buffered saline (placebo, n = 9) or 200 million mesenchymal stem cells (MSC, n = 13) 12 weeks after myocardial infarction (MI). Cardiac magnetic resonance and MDCT acquisitions were performed before randomization (12 weeks after MI induction) and at the study endpoint 24 weeks after MI induction. None of the animals received medication to control the intrinsic heart rate during first-pass acquisitions for assessment of LV volumes and LVEF. Delayed-enhancement MDCT imaging was performed 10 min after contrast delivery. Two blinded observers analyzed MDCT acquisitions.

RESULTS MDCT demonstrated that MSC therapy resulted in a reduction of infarct size from 14.3 ± 1.2% to 10.3 ± 1.5% of LV mass ($p = 0.005$), whereas infarct size increased in nontreated animals (from 13.8 ± 1.3% to 16.5 ± 1.5%; $p = 0.02$) (placebo vs. MSC; $p = 0.003$). Both observers had excellent agreement for infarct size ($r = 0.96$; $p < 0.001$). LVEF increased from 32.6 ± 2.2% to 36.9 ± 2.7% in MSC-treated animals ($p = 0.03$) and decreased in placebo animals (from 33.3 ± 1.4% to 29.1 ± 1.5%; $p = 0.01$; at week 24: placebo vs. MSC; $p = 0.02$). Infarct size, end-diastolic LV volume, and LVEF assessed by MDCT compared favorably with those assessed by cardiac magnetic resonance acquisitions ($r = 0.70$, $r = 0.82$, and $r = 0.902$, respectively; $p < 0.001$).

CONCLUSIONS This study demonstrated that cardiac MDCT can be used to evaluate infarct size, LV volumes, and LVEF after intramyocardial-delivered MSC therapy. These findings support the use of cardiac MDCT in preclinical and clinical studies for novel myocardial therapies. (J Am Coll Cardiol Img 2011;4:1284–93) © 2011 by the American College of Cardiology Foundation

From the *Department of Medicine, Division of Cardiology, Johns Hopkins University, Baltimore, Maryland; †Division of Cardiology, College of Medicine, Fondazione IRCCS, Azienda Ospedaliera San Paolo, Polo Universitario, Milan, Italy; ‡Department of Radiology, Uslan University Hospital, University of Ulsan College of Medicine, Uslan, South Korea; and the §Department of Biomedical Engineering, Johns Hopkins University, Baltimore, Maryland. All authors have reported that they have no relationships relevant to the contents of this paper to disclose.

Manuscript received July 8, 2011; revised manuscript received August 29, 2011, accepted September 2, 2011.

Cardiac imaging techniques play a critical role in the evaluation of novel therapies providing reliable surrogate endpoints in the ongoing effort to explore new approaches to treat heart diseases. Myocardial transplantation of different cell types and preparations has been widely investigated as a potential therapy for myocardial infarction (MI) and heart failure (HF) in recent years (1). Cardiac magnetic resonance (CMR) is one of the preferred imaging tools, in addition to the frequently used echocardiography and nuclear techniques, to provide reliable assessment of left ventricular ejection fraction (LVEF) and infarct size, which are generally accepted surrogate endpoints (2,3). Previous animal studies using CMR showed that mesenchymal stem cells (MSC) reduced infarct size and improved left ventricular (LV) function in acute and chronic MI (4–6). However, the use of CMR in the clinical setting is limited in patients with metallic implants and pacemakers and is relatively complex and time consuming.

Over the last decade, multidetector computed tomography (MDCT) has emerged as a novel tomographic cardiac imaging modality. Improvement in spatial and temporal resolution has allowed the implementation of myocardial applications, which are necessary to evaluate regenerative therapies. Although these MDCT applications are still investigative, current MDCT technology is able to provide reliable and reproducible assessment of cardiac function (7,8), myocardial viability with delayed contrast enhancement (DCE) (9–11), and myocardial blood flow (MBF) (12–14). However, whether MDCT can be used for follow-up studies and is able to show therapeutic effects of regenerative cell therapies has not been investigated. Accordingly, the purpose of this study was to 1) use MDCT LV function and myocardial viability as surrogate endpoints in a randomized animal study to evaluate outcomes of intramyocardial-delivered cell therapy and 2) evaluate the robustness and comparability of MDCT in relation to CMR.

METHODS

Animal model. All animal studies were approved by the Johns Hopkins University Institutional Animal Care and Use Committee and complied with the "Guide for the Care and Use of Laboratory Animals" (National Institutes of Health publication 80-23, revised 1985). Thirty-three female Göttingen minipigs were purchased from Marshall BioResources (North Rose, New York). MIs were induced by occlusion of the mid-left anterior descending artery with an inflated coronary angioplasty balloon as previously described (15). Five animals did not survive the infarct procedure. Two animals died during the early follow-up in the first 4 days after MI induction, and 4 animals died between weeks 8 and 12 post-MI. Therefore, a total of 22 animals were used in the study.

Cell harvest and isolation. The 13 animals randomized to cell therapy received bone marrow–derived porcine MSC. MSC were obtained, isolated, and expanded as previously described (6). In brief, MSC were harvested when they reached 80% to 90% confluence. Cells were placed in cryo bags at a concentration of 10 to 15 million MSC/ml and then frozen in a control-rate freezer to −180°C until the day of implantation. Trypan blue staining was performed to attest viability of thawed MSC lots before injection. Only MSC lots containing 85% or more of viable cells were used in the study.

Cell transplantation procedures. Twelve weeks after MI, animals were randomized to receive either intramyocardial injections of porcine MSC or phosphate-buffered saline to serve as a treatment (n = 13) or placebo (n = 9) group, respectively. Myocardial injections were performed as previously described (5,6).

Cardiac MDCT. MDCT images were acquired at 2 time points, before randomization at week 12 post-MI and 12 weeks after the intramyocardial injection procedure at week 24.

ABBREVIATIONS AND ACRONYMS

CMR = cardiac magnetic resonance

DCE = delayed contrast enhancement

HF = heart failure

LV = left ventricle/ventricular

LVEDV = left ventricular end-diastolic volume

LVEF = left ventricular ejection fraction

LVESV = left ventricular end-systolic volume

MBF = myocardial blood flow

MDCT = multidetector computed tomography

MI = myocardial infarction

MSC = mesenchymal stem cells

IMAGE ACQUISITION. Each animal was scanned with electrocardiographic (ECG) monitoring using a 0.5 mm × 64-slice MDCT scanner (Aquilion 64, Toshiba Medical Systems Corporation, Otawara, Japan). Data acquisition for LV function parameters and LV volumes were initiated manually at a threshold value of 180 Hounsfield units in the descending aorta. A 60-ml bolus of iodixanol (Visipaque 320 mg iodine/ml, Amersham Health, Buckinghamshire, United Kingdom) was injected intravenously at rate of 5.0 ml/s, opacifiying the LV chamber during first pass. An additional 90 ml of iodixanol was given intravenously after first-pass acquisitions, and DCE images were acquired 10 min after initial contrast delivery; 150 ml of iodixanol (0.91 ± 0.04 × 103 mg iodine/kg body weight) is 1.5 times the

human equivalent dose of contrast currently used for MDCT angiography.

During MDCT acquisition, respiration was suspended and imaging was performed using a retrospective ECG-gated MDCT protocol without dose modulation. Imaging parameters: gantry rotation time = 400 ms; detector collimation = 0.5 mm × 64 (isotropic voxels = 0.5 × 0.5 × 0.5 mm^3 − 13 linepairs/cm); helical pitch = variable depending on heart rate (range 6.4 to 6.8); tube voltage = 120 kV; and tube current = 400 mA. Animals with heart rates >100 beats/min during first-pass acquisition received intravenous metoprolol (2 to 5 mg) and /or amiodarone (50 to 150 mg) to achieve lower heart rate for DCE acquisitions.

IMAGE RECONSTRUCTION AND ANALYSIS. All raw data were reconstructed at contiguous 0.5-mm slice thickness by an adaptive multisegment reconstruction algorithm (16). First-pass acquisitions were reconstructed in 10% steps from 0% to 90% throughout the entire R-R interval using a standard kernel (FC43); images were reformatted at 4-mm slice thickness in short axis and evaluated in QMass CT 7.1 (Medis Medical Imaging Systems, Leiden, the Netherlands). Endocardial and epicardial borders of the LV were defined in all 10 contiguous slices, and each end-diastolic and end-systolic frame was determined to calculate LVEF, left ventricular end-diastolic volume (LVEDV), left ventricular end-systolic volume (LVESV), LV stroke volume, and LV remodeling parameters. The temporal resolution based on gantry rotation of all MDCT acquisitions was 211.5 ± 5.4 ms.

DCE-MDCT data (for myocardial scar assessment) were reconstructed at 80% of the R to R′ interval using the FC43 kernel and multisegment reconstruction. ECG editing to account for arrhythmias was performed when necessary. Multiplanar reformation at 4-mm slice thickness in the short axis of the heart was implemented, and MDCT images were analyzed using a custom research software package (Cine Tool, GE Medical Systems, Waukesha, Wisconsin). Infarct mass/volumes in DCE-MDCT images were defined by 3 SD of the signal intensity above the viable myocardium for the core infarct and 2 SD for the peri-infarct zone as described (16). Infarct size was defined as infarct mass as a percentage of LV mass. Both datasets, the cine MDCT acquisitions, and DCE-MDCT images, were analyzed by 2 blinded observers.

CMR imaging. CMR was performed at the same time points as MDCT imaging in random order on a 1.5-T MR scanner (CV/i, GE Medical Systems).

IMAGE ACQUISITION. LVEF function and LV volumes were assessed using a steady-state free precession pulse sequence (17). Six to 8 contiguous short-axis slices were prescribed to cover the entire LV, from base to apex. Image parameters were as follows: repetition time/echo time = 4.2 ms/1.9 ms; flip angle = 45°; 256 × 160 matrix; 8-mm slice thickness/no gap; 125 kHz; 28-cm field of view, and 1 number of signals averages. After an intravenous injection of gadolinium–diethylene triamine pentaacetic acid (0.2 mmol/kg body weight, Magnevist, Berlex, Wayne, New Jersey), DCE-CMR images were acquired 15 min later using an ECG-gated, breath-hold, interleaved, inversion recovery, and fast gradient echo pulse sequence. DCE-CMR images were acquired in the same location as the short-axis cine images. Imaging parameters were repetition time/echo time/inversion time = 7.3 ms/3.3 ms/180 to 240 ms; flip angle = 25°; 256 × 196 matrix; 8-mm slice thickness/no gap; 31.2 kHz; 28-cm field of view, and 2 number of signal averages. Inversion recovery time was adjusted as needed to null the normal myocardium (16).

IMAGE ANALYSIS. Cine MR images were analyzed with QMass MR 7.1 (Medis Medical Imaging Systems). To evaluate LVEF, LV volumes and myocardial mass endocardial and epicardial borders were defined each in the end-diastolic and end-systolic frame in 25 to 30 contiguous slices, and LV parameters and volumes were calculated. The temporal resolution of the cine MR images was 21.6 ± 0.9 ms. DCE-CMR images were analyzed on the same custom research software package (Cine Tool, GE Medical Systems) as DCE-MDCT images. Infarct size, determined by infarct mass as a percentage of LV mass and infarct volume in DCE-CMR images, was defined with the same threshold method described for DCE-MDCT analysis.

Statistical analysis. All data are presented as mean ± SEM unless otherwise stated. For infarct size and infarct volume comparison, Pearson correlation and linear regression analysis were used to compare MDCT and CMR. Results were confirmed by Bland-Altman analysis and agreement expressed as mean ± SD difference between methods at 95% confidence intervals. The MDCT and CMR data were evaluated with a paired Student *t* test. All analyses were performed in MedCalc (MedCalc

Software, Mariakerke, Belgium). A value of $p < 0.05$ was considered significant.

RESULTS

Baseline conditions. Twenty-two animals were used in this study 12 weeks after MI induction (91.9 ± 2.6 days and 87.9 ± 2.0 days after MI induction for placebo and MSC groups, respectively; $p = 0.19$). After randomization, animals in both groups were of similar age (16.8 ± 0.7 months and 15.5 ± 1.1 months for placebo and MSC, respectively; $p = 0.35$) and body weight (39.3 ± 1.6 kg and 35.7 ± 1.9 kg for placebo and MSC, respectively; $p = 0.11$).

Infarct size and scar volume. One placebo- and 2 MSC-treated animals were excluded from analysis due to poor imaging quality caused by motion artifacts at week 24. Infarct size, defined as infarct mass as percentage of LV mass, was reduced in all MSC-treated animals at week 24, whereas infarct size increased in all animals in the placebo group (Fig. 1). We observed a mean expansion of 29.1 ± 5.7% in infarct scar volume in the placebo group ($p = 0.001$). MSC therapy had limited effect on total scar volume ($p = 0.1$) (Figs. 1, 2C, and 2D). At week 24, infarct size and infarct volume were reduced in MSC-treated animals compared with those in the placebo group ($p = 0.003$ and $p = 0.01$, respectively), (Table 1, Figs. 2A to 2D).

Global LV function and LV volumes. Cardiac MDCT demonstrated that the decrease in infarct size resulted in 14.0 ± 6.7% improvement in LVEF in animals randomized to MSC therapy, whereas LVEF decreased by 12.3 ± 3.1% in the placebo group (Table 1, Figs. 2E and 2F). Of note, 2 animals that received MSC therapy did not show improved LVEF (Fig. 2F). All MDCT data for global LV function and LV volumes are summarized in Table 1.

Interobserver variability. Interobserver correlation for infarct size, total infarct volume, LVEF, and LVEDV were excellent ($r = 0.96$, $r = 0.98$, $r = 0.93$, and $r = 0.93$, respectively) in MDCT acquisitions. The complete data are presented in Table 2.

MDCT comparison with CMR. MDCT and CMR were performed on the same day in random order within 2 h following the first imaging study. Three animals had to be excluded from the analysis because CMR image data were not obtained on the day of the MDCT imaging. In 32 CMR studies, available the same day as MDCT acquisitions, we found fair agreement for infarct size, infarct volume, LVEF, and LVEDV (Fig. 3, Table 3). In addition, LVESV showed a good correlation with both imaging modalities ($r = 0.81$; $p < 0.001$). Bland-Altman analysis revealed a slight overestimation by 1.4 ml (95% confidence intervals: 16.3 to −13.6) with MDCT. Table 4 shows a direct comparison of all MDCT and MRI values at the 2 time points.

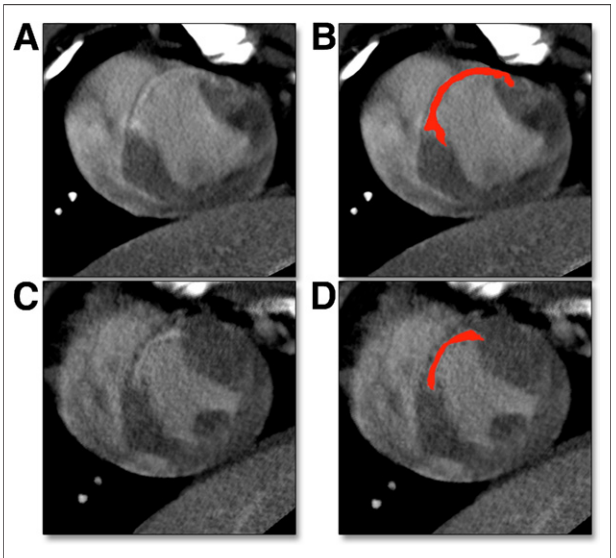

Figure 1. Infarct Assessment With DCE-MDCT

Example of delayed contrast enhancement multidetector computed tomography (DCE-MDCT) images for a placebo-treated **(A and B)** and a mesenchymal stem cell (MSC)–treated **(C and D)** animal at 24 weeks. DCE images were reconstructed in the short axis at 4-mm slice thickness. **(B and D)** show the slices of the placebo-treated **(A)** and MSC-treated **(C)** animals, respectively, with a computer-generated mask depicting the infarct area in **red**.

Finally, we showed that MDCT and CMR demonstrate similar effectiveness of MSC therapy from week 12 to week 24 (Fig. 4). Infarct size decreased by mean values of 4.7 ± 1.1 ml and 6.2 ± 2.0 ml when evaluated with DCE-MDCT and DCE-CMR in MSC-treated animals, respectively ($p = 0.43$). The changes in LVEF with MSC treatment were also apparent with both imaging modalities, with comparable mean values (4.5 ± 1.0 ml and 5.6 ± 1.3 ml, MDCT vs. MRI, respectively; $p = 0.4$). The changes between the placebo- and MSC-treated animals were also detected with both imaging modalities. Although the detected differences between MDCT and MRI were not significant for all infarct and functional parameters, the changes over time correlated with the assessment (Fig. 4).

DISCUSSION

This is the first study to use cardiac MDCT for the evaluation of therapeutic effects of cell therapy on

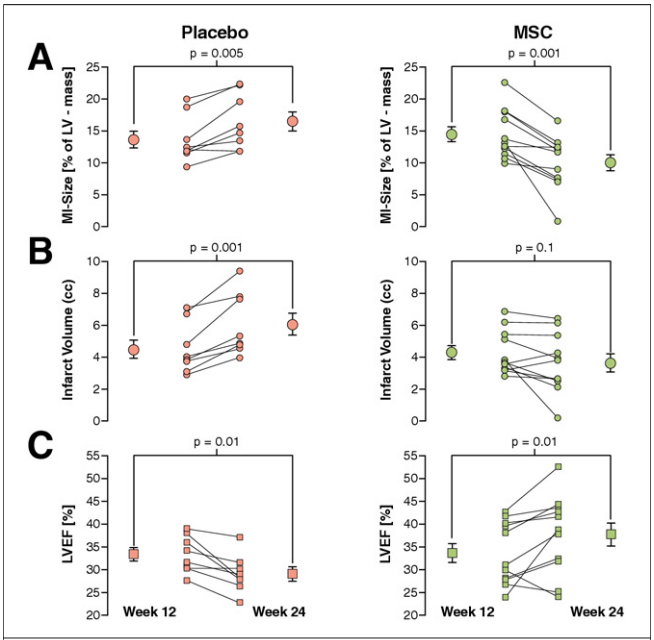

Figure 2. Impact of MSC Therapy Assessed by MDCT

All placebo animals (n = 8) showed an increase in infarct size **(A)** and infarct volume **(C)** at week 24, whereas intramyocardial delivery of MSC reduced infarct size **(B)** and stabilized infarct volume **(D)** in all treated animals (n = 11). **(E and F)** Left ventricular ejection fraction (LVEF) was decreased at week 24 in placebo animals, whereas it increased in most MSC-treated animals; however, the treatment failed to improve LVEF in 2 animals. MI = myocardial infarction; other abbreviations as in Figure 1.

infarct size, LV volumes, and LV function. Our results suggest that MDCT imaging reliably assessed LVEDV, LVEF, infarct size, and infarct volumes with DCE acquisitions; MDCT imaging was able to assess the effect of intramyocardial-delivered cell therapy compared with placebo. These findings confirmed previous studies that used CMR to evaluate the therapeutic potential of intramyocardial-delivered MSC in animals with HF with chronic infarct scars (6,18). This study introduces MDCT imaging as an alternative cardiac imaging technique to determine efficacy of novel myocardial therapeutics.

Table 1. Infarct Values, LV Function, and LV Volumes by MDCT

Parameter	Group	Week 12	Week 24	p Value
Infarct size, % of LV mass	Placebo	13.8 ± 1.3	16.3 ± 1.6	0.005
	MSC	14.3 ± 1.2	9.9 ± 1.3*	0.001
Total infarct volume, ml	Placebo	4.7 ± 0.6	6.2 ± 0.7	0.001
	MSC	4.4 ± 0.4	3.6 ± 0.5†	0.1
LVED mass, g	Placebo	33.6 ± 1.1	37.5 ± 1.6	0.02
	MSC	30.6 ± 1.3	37.4 ± 2.1‡	0.0003
LV ejection fraction, %	Placebo	33.3 ± 1.4	29.1 ± 1.5	0.01
	MSC	32.6 ± 2.2	36.9 ± 2.7§	0.03
Stroke volume, ml	Placebo	19.7 ± 1.6	19.4 ± 0.8	0.81
	MSC	15.1 ± 0.7	20.6 ± 1.6‡	0.004
LVEDV, ml	Placebo	60.1 ± 5.7	67.6 ± 4.1	0.16
	MSC	48.1 ± 3.1	56.3 ± 4.3‡	0.01
LVESV, ml	Placebo	40.4 ± 4.5	48.3 ± 3.7	0.07
	MSC	33.0 ± 2.9	36.4 ± 4.1‖	0.15

Values are mean ± SEM. MSC (n = 11) versus placebo (n = 8). *p = 0.003. †p = 0.01. ‡p = nonsignificant. §p = 0.02. ‖p = 0.047.
LV = left ventricular; LVED = left ventricular end-diastolic; LVEDV = left ventricular end-diastolic volume; LVESV = left ventricular end-systolic volume; MDCT = multidetector computed tomography; MSC = mesenchymal stem cell.

Myocardial infarct scar assessment by MDCT. MDCT has the capability to distinguish between viable and nonviable myocardium with DCE for the detection of acute and chronic infarct scars, and its use has recently been reported in animal experiments and human studies; however, it is still considered an investigative technique (9–11,16,19). After intravenous delivery, iodine-based contrast agents accumulate in myocardial tissue damaged by MI. The discrimination between viable and nonviable myocardium results from increased attenuation values caused by the accumulation of iodine molecules in the infarct area detected by MDCT. This is in contrast to enhancement mechanisms by CMR that rely on alteration of the contrast media via interactions with water molecules (9). The infarct sizes detected by DCE-MDCT in this study were significantly smaller than matching CMR values; these results are in accordance with previously published data for acute and chronic MI (16,20). Thus, DCE-MDCT– and DCE-CMR–derived values for infarct size and infarct volume should not be used interchangeably at the current status of MDCT technology.

The extent of contrast enhancement detected by CMR has been shown to predict the response to medical treatment in patients with HF (21). Reduction of infarct size has been noted with DCE-CMR following myocardial cell therapy in animal studies and patients (4–6,22,23). Thus, quantification of infarct size and infarct volume by DCE-MDCT could be a valuable surrogate endpoint, allowing the prediction of response to therapy. DCE-MDCT currently offers the highest spatial resolution for transmural characterization of infarct scars, and this can be particularly helpful in guiding intramyocardial delivery of cell-based therapies. An akinetic segment might be deemed nonviable by nuclear techniques using limited spatial resolution but shows some viability in DCE-MDCT, which increases the likelihood that this segment will eventually recover with therapeutic intervention (24).

Table 2. Interobserver Variability for MDCT

Parameters	Correlation Coefficient (r)	95% CI for r	Significance Level (p Value)	Difference (Mean)	95% CI for Mean
Infarct size, % of LV mass	0.96	0.93–0.98	<0.0001	0.6	3.0 to −1.8
Infarct volume, ml	0.98	0.95–0.99	<0.0001	0.05	0.8 to −0.7
LVED mass, g	0.84	0.71–0.92	<0.0001	−0.9	3.9 to −5.7
LV ejection fraction, %	0.93	0.87–0.96	<0.0001	−1.1	4.8 to −7.0
Stroke volume, ml	0.84	0.70–0.91	<0.0001	−0.1	5.2 to −5.3
ED volume, ml	0.92	0.84–0.96	<0.0001	3.1	14.9 to −8.7
ES volume, ml	0.93	0.86–0.96	<0.0001	3.2	12.7 to −6.2

CI = confidence interval; ED = end-diastolic; ES = end-systolic; other abbreviations as in Table 1.

Evaluation of cardiac function and volumes by MDCT. Evaluation of cardiac function with MDCT is accomplished with intravenous injection of iodine-based contrast agents for opacification of the blood pool to delineate the borders of the ventricle and application of retrospective ECG-gated protocols to record the complete cardiac cycle during the R-R interval. Various investigators have reported a consistent overestimation of LVESV and an underestimation of LVEF by MDCT with 4-slice and early 16-slice technology compared with CMR; however, with the introduction of 64-slice MDCT technology and improvement in temporal resolution, these intermethod differences in global LV function variables are no longer reproduced. Temporal resolution, based on gantry rotation, has been reported to be less than 165 ms with single-source systems and 83 ms with dual-source MDCT technology (7). Our results are in accordance with studies comparing single-source and dual-source 64-slice MDCT—with CMR showing small differences between both modalities and narrow Bland-Altman windows (25–29). In our study, we observed good correlation coefficients for LVEDV and LVEF, and we were able to confirm the linear relationship between both volumetric imaging techniques for LV function and LV remodeling parameters, making both tomographic imaging methods interchangeable for LV function and LV volume assessment.

Evaluation of the cardiac structure, LV volumes, and LV function—specifically LVEF—is an integral step in determining prognosis and therapy for patients with HF (30). Human trials, using a variety of cell-therapy approaches, have used improve-

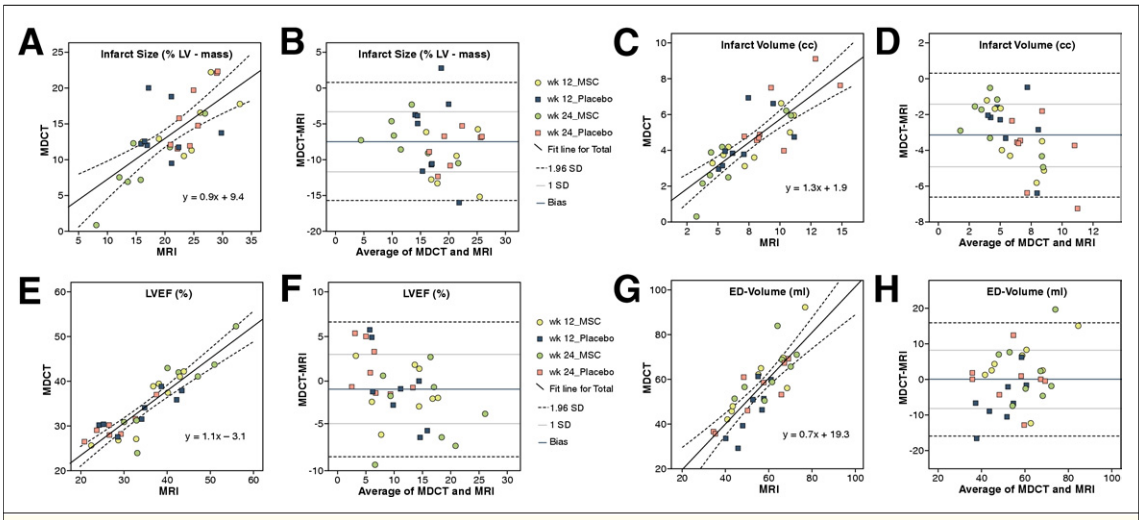

Figure 3. Quantitative Assessment of MDCT and CMR Values

The relation between MDCT and cardiac magnetic resonance (CMR) for infarct size, infarct volume, LVEF, and LV end-diastolic (ED) volume was evaluated for 16 animals at both time points. **(A and B)** MDCT and CMR showed a fair correlation for infarct size at 4-mm and 8-mm slice thickness, respectively, with an underestimation of infarct size by DCE-MDCT compared with DCE-CMR in Bland-Altman analysis. **(C and D)** Good correlation of infarct volume with less underestimation by DCE-MDCT than that for infarct size. **(E and F)** Good correlation of both modalities with minimal underestimation of LVEF by MDCT. **(G and H)** MDCT and CMR show excellent correlation of ED volume. Abbreviations as in Figures 1 and 2.

Table 3. Correlation and Bland-Altman Analysis of MDCT and CMR

Parameters	Correlation Coefficient (r)	Linear Regression Equation	Significance Level (p Value)	Mean Difference (Bias)	SD	95% CI for Mean
Infarct size, % LV mass						
Total	0.70	y = 0.9x + 9.4	<0.0001	−7.5	4.27	0.8 to −15.9
Week 12	0.37	y = 0.5x + 14.1	0.16	−7.5	5.23	3.0 to −18.0
Week 24	0.89	y = 1.0x + 7.5	<0.0001	−7.5	3.06	−1.7 to −13.3
Placebo	0.44	y = 0.5x + 15.4	0.09	−7.4	4.22	1.7 to −16.5
MSC	0.82	y = 1.1x + 6.1	<0.001	−7.6	4.07	0.2 to −15.4
Total infarct volume, ml						
Total	0.81	y = 1.3x + 1.9	<0.0001	−3.2	1.71	0.3 to −6.6
Week 12	0.68	y = 1.2x + 2.3	0.004	−3.0	1.77	0.3 to −6.4
Week 24	0.87	y = 1.3x + 1.9	<0.0001	−3.3	1.76	0.3 to −6.9
Placebo	0.73	y = 1.1x + 2.7	0.001	−3.3	1.94	0.4 to −7.0
MSC	0.86	y = 1.5x + 1.2	<0.0001	−3.0	1.53	0.3 to −6.2
LV ejection fraction, %						
Total	0.90	y = 1.1x − 3.2	<0.0001	−0.9	3.81	6.6 to −8.5
Week 12	0.87	y = 1.1x − 2.4	<0.0001	−0.9	3.69	6.1 to −8.0
Week 24	0.92	y = 1.1x − 3.5	<0.0001	−0.9	4.19	7.3 to −9.1
Placebo	0.88	y = 1.4x − 12.1	<0.0001	0.3	3.43	7.6 to −7.0
MSC	0.91	y = 1.0x − 3.6	<0.0001	−2.2	3.78	5.0 to −9.6
ED volume, ml						
Total	0.82	y = 0.7x + 19.3	<0.0001	−0.02	6.63	15.9 to −16.0
Week 2	0.84	y = 0.6x + 23.6	<0.001	−1.2	5.90	15.7 to −18.0
Week 24	0.81	y = 0.8x + 12.2	<0.001	1.1	7.44	16.3 to −14.1
Placebo	0.81	y = 0.7x + 18.5	<0.001	−3.1	6.38	11.1 to −17.3
MSC	0.81	y = 0.7x + 15.9	<0.001	3.0	7.10	18.8 to −12.7

Total: n = 32; week 12, week 24, placebo, MSC: n = 16.
CMR = cardiac magnetic resonance; other abbreviations as in Tables 1 and 2.

ments in LVEF as an endpoint (3). Compared with volumetric changes, using LVEF as an endpoint has the advantage of denoting a survival difference and is an accepted surrogate measure for mortality (31). The magnitude of treatment effect on LVEF seen in these trials has ranged from 5% to 9%, whereas the change in the control groups has ranged from −2% to 4% (32).

Advantages and limitations of MDCT imaging. As a novel cardiac imaging option for LV function and viability, MDCT offers some solutions for the difficulties faced in CMR. MDCT can be safely performed in patients with metallic implants, such as pacemakers, defibrillators, and prostheses, who are inappropriate candidates for CMR. Although CMR is considered the reference standard for cardiac function and myocardial viability—based on the accuracy and reproducibility of measurements—the duration of CMR acquisitions with multiple prolonged breath-holds are required to obtain adequate datasets, are time consuming, and are impossible in patients with claustrophobia. Thus, CMR is limited to specialized centers, which is in contrast to the widely accessible cardiac MDCT. MDCT imaging is fast and offers good temporal and excellent spatial resolution; however, MDCT acquisitions require iodinated contrast agents and involve radiation exposure.

Future perspective. To translate cardiac function and viability assessment with MDCT into clinical trials, standardized low-dose protocols are needed, especially to minimize overall radiation exposure because follow-up studies are required for outcome assessment. In the latest generation of MDCT scanners, ECG-gated tube current modulations are commonly applied in retrospective acquisitions for evaluation of cardiac function (7). Low-dose DCE protocols have been reported (9). We recently described a prospectively gated protocol for high-resolution DCE-MDCT imaging that lowered the radiation dose by an order of magnitude (33).

In addition to cardiac function and viability, MDCT is able to assess MBF. Cardiac CT perfusion is based on the same first-pass principle as CMR (14), which has been used to evaluate cell therapy (5). Semiquantitative and quantitative as-

Table 4. Comparison of MDCT and CMR Studies (N = 32)

Parameter	Groups	Placebo			MSC		
		Week 12	Week 24	p Value	Week 12	Week 24	p Value
Infarct size, % of LV mass	MDCT	13.8 ± 1.3	16.3 ± 1.6	0.02	14.5 ± 1.4	9.4 ± 1.7*	0.005
	CMR	20.1 ± 1.6	24.9 ± 1.1	0.03	23.3 ± 2.1	15.8 ± 2.0†	0.01
Total infarct volume, ml	MDCT	4.5 ± 0.5	5.9 ± 0.7	0.002	4.4 ± 0.5	3.5 ± 0.7‡	0.04
	CMR	7.1 ± 0.8	9.9 ± 0.9	0.03	7.8 ± 0.9	6.0 ± 1.1‡	0.04
LVED mass, g	MDCT	35.0 ± 1.4	37.8 ± 1.4	0.08	33.5 ± 1.6	39.4 ± 2.8	0.10
	CMR	37.3 ± 2.5	41.3 ± 2.4	0.16	32.2 ± 1.9	37.8 ± 1.4	0.05
LV ejection fraction, %	MDCT	33.3 ± 1.4	29.1 ± 1.5	0.03	34.7 ± 2.5	38.5 ± 3.2§	0.02
	CMR	34.0 ± 2.6	27.8 ± 1.9	0.01	35.9 ± 2.6	41.7 ± 3.3‖	0.02
ED volume, ml	MDCT	60.1 ± 5.7	67.6 ± 4.1	0.16	48.7 ± 4.0	54.7 ± 3.8¶	0.44
	CMR	56.6 ± 4.7	65.1 ± 2.5	0.08	50.2 ± 3.5	53.5 ± 4.69¶	0.67

Week 24: MSC (n = 8) versus placebo (n = 8). *p = 0.01. †p = 0.001. ‡p = 0.03. §p = 0.02. ‖p = 0.003. ¶p = 0.04.
Abbreviations as in Tables 1, 2, and 3.

sessments of MBF with MDCT have been reported in experimental animals (9,13). Cardiac MDCT is poised to offer a comprehensive evaluation of novel myocardial therapeutics.

Study limitations. This animal study was conducted without any medical therapy given to patients after MI. Therefore, the chronic MIs expanded and the infarct size increased in the placebo group, consis-

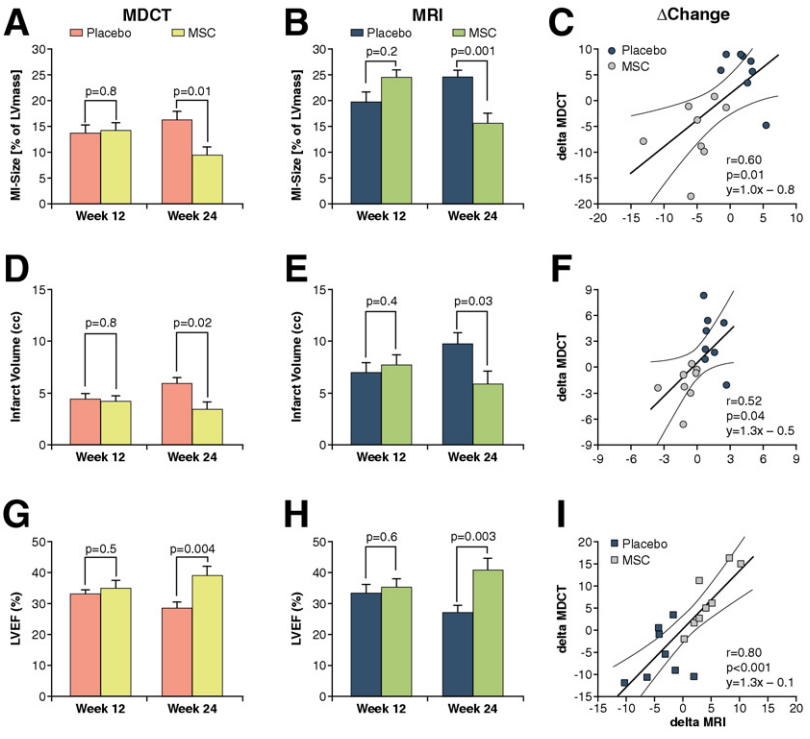

Figure 4. Comparison of MDCT and CMR Values for MI and LVEF Assessment

Data of placebo- (n = 8) and MSC-treated (n = 8) animals imaged on the same day with both modalities were compared to evaluate the absolute difference of MDCT and MRI values, effectiveness of MSC therapy, and correlation of the evaluated changes over time (Δchange). **(A and B)** Both DCE-MDCT and DCE-CMR detected significant differences of infarct size with MSC therapy ($p < 0.0001$). **(C)** The changes over time showed a fair correlation between MDCT and CMR assessment. **(D to F)** These differences were also apparent as infarct volume was compared ($p < 0.0001$), showing a modest correlation of both modalities. **(G and H)** Values for LVEF were similar with MDCT and CMR. Importantly, the effectiveness of MSC therapy was apparent with both imaging modalities, and detected changes were not significantly different between MDCT and CMR evaluations in the studied animals ($p = 0.06$). **(I)** The Δchange analysis showed a good correlation for LVEF evaluation with MDCT and CMR. Abbreviations as in Figures 1, 2, and 3.

tent with results from a clinical study using noninvasive imaging techniques conducted in the early 1980s (34). With modern medical therapy, decreases in infarct size are anticipated in chronic MI, as shown in a recent CMR study (35). To complicate matters, additive effects of angiotensin-converting enzyme inhibition with beta-blockade in combination with cell therapy have been described (36). Although these limitations are evident in the current study, the goal of this study was to demonstrate the usefulness of MDCT to evaluate the effect of myocardial therapies.

However, there are some limitations that may affect the transfer of the reported MDCT protocols and results to human trials. First, the animals presented had elevated heart rates, which are usually considered a relative contraindication for MDCT. Although the reported MDCT protocols proved reliable even under these unfavorable conditions, patients with elevated heart rates above 60 to 70 beats/min may receive negative chronotropic medication to reduce the heart rate for coronary CT angiography. This will affect the value of functional analysis because ventricular volumes change if beta-blockers are applied; however, beta-blockers only have to be given if coronary CT angiography is mandated. Second, no tube current modulation was applied, as is routinely done now in patient studies to reduce radiation exposure. Increased image noise on systolic images of ECG-gated tube current modulation may affect the accuracy of global and regional LV function assessment. Third, because of the passive contrast kinetics of iodine-based contrast agents and the limited collateral circulation in pigs, DCE-MDCT imaging of chronic infarct scars in this animal model required a relatively large dose of iodine to cause a sufficient change in the volume distribution in the myocardial bed. In this study, we used 1.5 times a human equivalent dose, although successful viability imaging in humans has been reported in several studies with standard contrast volumes used for coronary CT angiography (37).

CONCLUSIONS

This animal study suggests that cardiac MDCT can be reliably used to evaluate infarct size, infarct volumes, LV volumes, and LV function after intramyocardial-delivered MSC therapy with sensitivity similar to CMR and showing similar changes at follow-up. These findings support the use of cardiac MDCT in preclinical and clinical studies as a noninvasive imaging technique for detecting therapeutic effects of novel myocardial therapies.

Reprint requests and correspondence: Drs. Karl H. Schuleri and Albert C. Lardo, Image Guided Cardiotherapy Laboratory, Johns Hopkins School of Medicine, Division of Cardiology, 1042 Ross Building, Baltimore, Maryland 21205. *E-mail: al@jhmi.edu and kschuleri@jhmi.edu.*

REFERENCES

1. Wollert KC, Drexler H. Cell therapy for the treatment of coronary heart disease: a critical appraisal. Nat Rev Cardiol 2010;7:204–15.
2. Lau JF, Anderson SA, Adler E, Frank JA. Imaging approaches for the study of cell-based cardiac therapies. Nat Rev Cardiol 2010;7:97–105.
3. Beeres SL, Bengel FM, Bartunek J, et al. Role of imaging in cardiac stem cell therapy. J Am Coll Cardiol 2007;49:1137–48.
4. Amado LC, Saliaris AP, Schuleri KH, et al. Cardiac repair with intramyocardial injection of allogeneic mesenchymal stem cells after myocardial infarction. Proc Natl Acad Sci U S A 2005;102:11474–9.
5. Schuleri KH, Amado LC, Boyle AJ, et al. Early improvement in cardiac tissue perfusion due to mesenchymal stem cells. Am J Physiol Heart Circ Physiol 2008;294:H2002–11.
6. Schuleri KH, Feigenbaum GS, Centola M, et al. Autologous mesenchymal stem cells produce reverse remodelling in chronic ischaemic cardiomyopathy. Eur Heart J 2009;30:2722–32.
7. Sayyed SH, Cassidy MM, Hadi MA. Use of multidetector computed tomography for evaluation of global and regional left ventricular function. J Cardiovasc Comput Tomogr 2009;3:S23–34.
8. Savino G, Zwerner P, Herzog C, et al. CT of cardiac function. J Thorac Imaging 2007;22:86–100.
9. Schuleri KH, George RT, Lardo AC. Applications of cardiac multidetector CT beyond coronary angiography. Nat Rev Cardiol 2009;6:699–710.
10. Gerber BL, Belge B, Legros GJ, et al. Characterization of acute and chronic myocardial infarcts by multidetector computed tomography: comparison with contrast-enhanced magnetic resonance. Circulation 2006;113:823–33.
11. Lardo AC, Cordeiro MA, Silva C, et al. Contrast-enhanced multidetector computed tomography viability imaging after myocardial infarction: characterization of myocyte death, microvascular obstruction, and chronic scar. Circulation 2006;113:394–404.
12. George RT, Arbab-Zadeh A, Miller JM, et al. Adenosine stress 64- and 256-row detector computed tomography angiography and perfusion imaging: a pilot study evaluating the transmural extent of perfusion abnormalities to predict atherosclerosis causing myocardial ischemia. Circ Cardiovasc Imaging 2009;2:174–82.
13. George RT, Jerosch-Herold M, Silva C, et al. Quantification of myocardial perfusion using dynamic 64-detector computed tomography. Invest Radiol 2007;42:815–22.

14. Schuleri KH, George RT, Lardo AC. Assessment of coronary blood flow with computed tomography and magnetic resonance imaging. J Nucl Cardiol 2010;17:582–90.
15. Schuleri KH, Boyle AJ, Centola M, et al. The adult Gottingen minipig as a model for chronic heart failure after myocardial infarction: focus on cardiovascular imaging and regenerative therapies. Comp Med 2008;58:568–79.
16. Schuleri KH, Centola M, George RT, et al. Characterization of peri-infarct zone heterogeneity by contrast-enhanced multidetector computed tomography: a comparison with magnetic resonance imaging. J Am Coll Cardiol 2009;53:1699–707.
17. Slavin GS, Saranathan M. FIESTA-ET: high-resolution cardiac imaging using echo-planar steady-state free precession. Magn Reson Med 2002;48:934–41.
18. Quevedo HC, Hatzistergos KE, Oskouei BN, et al. Allogeneic mesenchymal stem cells restore cardiac function in chronic ischemic cardiomyopathy via trilineage differentiating capacity. Proc Natl Acad Sci U S A 2009;106:14022–7.
19. le Polain de Waroux JB, Pouleur AC, Goffinet C, Pasquet A, Vanoverschelde JL, Gerber BL. Combined coronary and late-enhanced multidetector-computed tomography for delineation of the etiology of left ventricular dysfunction: comparison with coronary angiography and contrast-enhanced cardiac magnetic resonance imaging. Eur Heart J 2008;29:2544–51.
20. Baks T, Cademartiri F, Moelker AD, et al. Multislice computed tomography and magnetic resonance imaging for the assessment of reperfused acute myocardial infarction. J Am Coll Cardiol 2006;48:144–52.
21. Bello D, Shah DJ, Farah GM, et al. Gadolinium cardiovascular magnetic resonance predicts reversible myocardial dysfunction and remodeling in patients with heart failure undergoing beta-blocker therapy. Circulation 2003;108:1945–53.
22. Britten MB, Abolmaali ND, Assmus B, et al. Infarct remodeling after intracoronary progenitor cell treatment in patients with acute myocardial infarction (TOPCARE-AMI): mechanistic insights from serial contrast-enhanced magnetic resonance imaging. Circulation 2003;108:2212–8.
23. Dill T, Schachinger V, Rolf A, et al. Intracoronary administration of bone marrow-derived progenitor cells improves left ventricular function in patients at risk for adverse remodeling after acute ST-segment elevation myocardial infarction: results of the Reinfusion of Enriched Progenitor Cells and Infarct Remodeling in Acute Myocardial Infarction study (REPAIR-AMI) cardiac magnetic resonance imaging substudy. Am Heart J 2009;157:541–7.
24. Kim RJ, Shah DJ. Fundamental concepts in myocardial viability assessment revisited: when knowing how much is "alive" is not enough. Heart 2004;90:137–40.
25. Annuar BR, Liew CK, Chin SP, et al. Assessment of global and regional left ventricular function using 64-slice multislice computed tomography and 2D echocardiography: a comparison with cardiac magnetic resonance. Eur J Radiol 2008;65:112–9.
26. Bruners P, Mahnken AH, Knackstedt C, et al. Assessment of global left and right ventricular function using dual-source computed tomography (DSCT) in comparison to MRI: an experimental study in a porcine model. Invest Radiol 2007;42:756–64.
27. Busch S, Johnson TR, Wintersperger BJ, et al. Quantitative assessment of left ventricular function with dual-source CT in comparison to cardiac magnetic resonance imaging: initial findings. Eur Radiol 2008;18:570–5.
28. Palumbo A, Maffei E, Martini C, et al. Functional parameters of the left ventricle: comparison of cardiac MRI and cardiac CT in a large population. Radiol Med;115:702–13.
29. Mahnken AH, Bruners P, Bornikoel CM, et al. Dual-source CT assessment of ventricular function in healthy and infarcted myocardium: an animal study. Eur J Radiol 2011;77:443–9.
30. Hunt SA, Abraham WT, Chin MH, et al. 2009 focused update incorporated into the ACC/AHA 2005 Guidelines for the Diagnosis and Management of Heart Failure in Adults: a report of the American College of Cardiology Foundation/American Heart Association Task Force on Practice Guidelines: developed in collaboration with the International Society for Heart and Lung Transplantation. J Am Coll Cardiol 2009;53:e1–90.
31. Rector TS, Cohn JN. Prognosis in congestive heart failure. Annu Rev Med 1994;45:341–50.
32. Fuster V, Sanz J, Viles-Gonzalez JF, Rajagopalan S. The utility of magnetic resonance imaging in cardiac tissue regeneration trials. Nat Clin Pract Cardiovasc Med 2006;3 Suppl 1:S2–7.
33. Chang HJ, George RT, Schuleri KH, et al. Prospective electrocardiogram-gated delayed enhanced multidetector computed tomography accurately quantifies infarct size and reduces radiation exposure. J Am Coll Cardiol Img 2009;2:412–20.
34. Erlebacher JA, Weiss JL, Eaton LW, Kallman C, Weisfeldt ML, Bulkley BH. Late effects of acute infarct dilation on heart size: a two dimensional echocardiographic study. Am J Cardiol 1982;49:1120–6.
35. Engblom H, Hedstrom E, Heiberg E, Wagner GS, Pahlm O, Arheden H. Rapid initial reduction of hyperenhanced myocardium after reperfused first myocardial infarction suggests recovery of the peri-infarction zone: one-year follow-up by MRI. Circ Cardiovasc Imaging 2009;2:47–55.
36. Boyle AJ, Schuster M, Witkowski P, et al. Additive effects of endothelial progenitor cells combined with ACE inhibition and beta-blockade on left ventricular function following acute myocardial infarction. J Renin Angiotensin Aldosterone Syst 2005;6:33–7.
37. Nieman K, Shapiro MD, Ferencik M, et al. Reperfused myocardial infarction: contrast-enhanced 64-section CT in comparison to MR imaging. Radiology 2008;247:49–56.

Key Words: CMR ■ delayed contrast enhancement ■ Göttingen minipig ■ heart failure ■ MDCT ■ mesenchymal stem cell ■ myocardial infarction.